Sixth International Symposium on Turbulence and Shear Flow Phenomena
Seoul, Korea, 22-24 June 2009

IMPACT OF REACTION AND LOCATION OF A PILOT JET ON THE FLOW STRUCTURES IN A CO-ANNULAR SWIRL BURNER

Ping Wang*
Institute for Technical Thermodynamics,
Karlsruhe University
Kaiserstraße 12, 76128 Karlsruhe, Germany
ping.wang@mailbox.tu-dresden.de

Jochen Fröhlich
Institute of Fluid Mechanics,
Technical University of Dresden
George-Bähr-Straße 3c, 01062 Dresden, Germany
jochen.froehlich@tu-dresden.de

ABSTRACT

The paper investigates the impact of heat release and pilot jet location on the swirling flow structures in a co-annular swirl burner without confinement. Two iso-thermal turbulent swirling flow cases and three turbulent premixed swirling flames are studied with the aid of large-eddy simulation. Two geometries are considered, one featuring a pilot lance flush with the outlet and one with retracted pilot lance. The Reynolds number is 35,000. Detailed comparisons with experimental data are performed for velocity statistics and generally good agreement is achieved. Furthermore, coherent structures are analyzed and local power spectra computed. In the non-reactive case with retracted pilot jet, a very strong precessing vortex core (PVC) is observed in both numerical results and the experiment. The PVC is weak in the non-retracted case. In the reactive cases where the whole central recirculation zone (CRZ) is enclosed in the high-temperature post-flame region, the PVC is almost completely suppressed.

INTRODUCTION

Turbulent swirling flows are important and widely used in energy production devices such as internal combustion engines, gas turbine combustors, industrial burners and boilers. A strong inlet swirl induces a central recirculation zone (CRZ) in the flowfield which, recirculates the hot combustion products and the radicals and anchors the flame at the burner. In lean premixed combustors, in addition to the CRZ, an extra pilot jet with richer mixture is often utilized for enhanced flame stabilization. In the resulting complex flow system, flow instabilities are observed in both experiments (Habisreuther, et al., 2006) and simulations (Fröhlich et al., 2008).

The ability to predict the size, shape and the position of the CRZ is essential to the prediction of turbulent swirling flows with and without reaction. Generally, the CRZ is not stable but precesses around the axis, hence termed precessing vortex core (PVC). The occurrence of a PVC in isothermal swirling flow depends on several factors such as swirl number and geometrical setup etc. Under combustion conditions its behaviour is dependent further on equivalence ratio, mode of fuel entry, flow rate, etc. Numerous studies have been reported on the influence of different parameters such as the level of swirl, the inflow profile, the flow configuration, Reynolds number, and heat release etc., as reviewed in (Lucca-Negro and Doherty, 2001; Syred, 2006).

The main objective of the present work is to investigate the impact of heat release and pilot jet location on the swirling flow structures in an unconfined co-annular swirl burner. To this end, two iso-thermal turbulent swirling flow cases and three turbulent premixed swirling flames are simulated using large-eddy simulation (LES).

NUMERICAL METHOD

To simulate the turbulent premixed combustion, the thickened-flame (TF) model (Colin et al., 2000) is employed. Although it is comparatively simple it has shown to perform well for the type of flow studied in this work (Selle et al., 2004). In the TF model, pre-exponential constants and transport coefficients are both modified by a factor F to yield a thicker reaction zone which can then be resolved on an LES mesh. The subgrid-scale wrinkling is accounted for by an efficiency function E related to the local subgrid-turbulent velocity and the filter width. The equation for the mass fraction of the kth species is thus modified to read

$$\frac{\partial \rho Y_k^{th}}{\partial t} + \frac{\partial \rho Y_k^{th} u_j}{\partial x_j} = \frac{\partial}{\partial x_j}(\rho D_k EF \frac{\partial Y_k^{th}}{\partial x_j}) + \frac{E}{F}\dot{\omega}_k(Y_j^{th}, T^{th}) \qquad (1)$$

where the superscript '*th*' represents thickened quantities. With this modification, the resolved flame propagates at a turbulent flame speed equal to E times the laminar flame speed, while the resolved flame thickness is F times the laminar flame thickness. The wrinkling function E is determined as proposed by Colin et al. (2000). The

* Currently a guest scientist at TU-Dresden

thickening factor F is a local quantity and generally estimated as

$$F(n) = n\Delta / \delta_L^0 \qquad (2)$$

where Δ is the characteristic grid cell length scale, and δ_L^0 is the laminar flame thickness. Hence, the thickened flame is resolved with n grid cells. An optimal value for the parameter n generally is in the range 5-10 (T. Poinsot, private communication). In the present work, the effect of n is studied, demonstrating that n=5 is a good choice for the flow cases under consideration. The dynamic procedure of (Legier et al., 2000) was used to determine F. It reduces F to unity remote from the flame and hence provides realistic transport coefficients there. To simulate the lean premixed methane/air combustion of the experiment, the two-step chemical scheme 2sCM2 (Selle et al., 2004) is used which takes into account six species (CH_4, O_2, CO_2, CO, H_2O and N_2) and two reactions:

(a) $CH_4 + 1.5O_2 \rightarrow CO + 2H_2O$

(b) $CO + 0.5\ O_2 \leftrightarrow CO_2$.

These models were implemented in the Finite-Volume code LESOCC2C (Wang et al., 2008 and 2009), solving the low-Mach number version of the compressible Navier-Stokes equations on block-structured body-fitted curvilinear grids.

BURNER SETUP AND COMPUTATIONAL DOMAIN

The investigated swirl burner by Büchner and his co-workers (2004) is sketched in Fig. 1a, together with the computational domain (not to scale). It consists of two co-annular swirling jets discharging into the ambient air which is at rest. The tube in the centre of this setup (indicated by gray color) is the pilot lance. The Reynolds number of the flow based on the bulk velocity U_b=11.5 *m/s*, and the radius of outer jet nozzle R=55 *mm*, is Re=35,000. The mass flow rates are 180 m^3/h and 20 m^3/h at normal condition, and the theoretical swirl numbers are 0.9 and 0.79 for the main and the pilot jet, respectively. Swirl is co-rotating. The blades of the axial swirl generator for the pilot jet used in the experiment were represented geometrically using 12 inclined blades as seen in Fig. 1b.

For the inflow of the main jet, 12 gaps where positioned regularly along the circumference of the cylindrical surface, with radial and tangential velocity component being imposed. Different swirl levels are achieved by adjusting the tangential velocity component and maintaining the radial velocity component. A slip condition was used on the outer boundary and a convective outflow condition was imposed at the exit. The Werner-Wengle wall function was employed at all solid walls. A very small uniform co-flow was imposed remote from the jets as validated in (García-Villalba, et al., 2006).

Two geometrical setups are studied: pilot jet flush with outlet (Fig. 1a) and pilot jet retracted by 40 *mm* (Fig. 1c). To study the impact of reaction and pilot jet location on the flow, five cases were simulated as listed in Table 1. In the reactive flow cases, the equivalence ratio is 0.667 and 0.833 for the main jet and pilot jet, respectively.

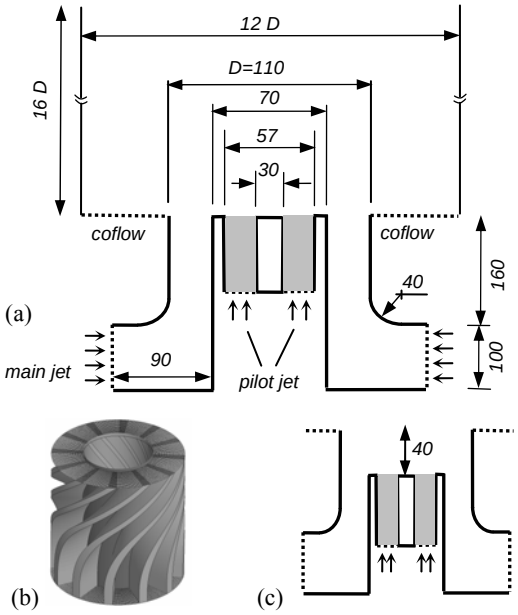

Fig. 1. (a) Sketch of the computational domain, pilot jet flush with main jet, units is *mm*. (b) 3D view of the pilot swirler located at the position indicated by gray color in part (a) and (c). (c) Pilot jet retracted by 40 *mm*.

Table 1: Overview over the cases simulated, definition in the text.

cases	Reactive	Retracted	n	Grid/10^6	Δt/μs	$r_{1/2}$
I00	no	no	/	8.45	6.69	1.4
I40	no	yes	/	8.88	6.69	1.6
R00	yes	no	5	4.34	2.84	2.0
R40	yes	yes	5	4.56	2.52	1.7
R40B	yes	yes	10	4.56	1.25	1.7

RESULTS AND DISCUSSION

Effect of Thickening-Factor

The influence of the parameter n in Eqn. 2 is visualized with Fig. 2, displaying instantaneous reaction rates from case R40 and R40B. With small n, more flame wrinkles are resolved, which indicates that the interaction between turbulence and flame is better resolved so that the contribution from the SGS wrinkling model is smaller. In addition to this, a number of 1D laminar flame simulations were performed with different values of n and aimed to compare the integral heat release across the flame front. It was found that the relative difference among the results obtained from the thickened flames with n=5 and n=10 and the DNS result is smaller than 0.6%. The main benefit with small n is the larger time step allowed in the computation (see Table 1).

Fig. 3 shows an instantaneous temperature field at the center plane obtained from case R40, and the corresponding distribution of the dynamic thickening-factor. It demonstrates that F is unity in the post flame zone and the unburnt region, but has large values in the flame brush to resolve the thickened flame with multiple grid cells.

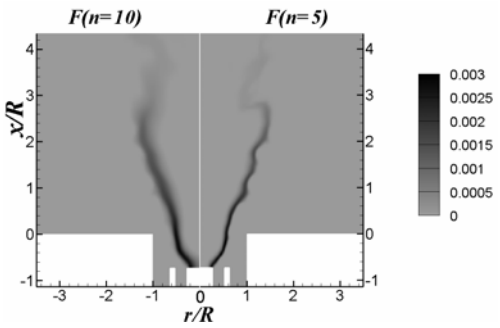

Fig. 2. The influence of the parameter n: contours of the instantaneous CH_4 reaction rate, for R40B (left) and R40 (right).

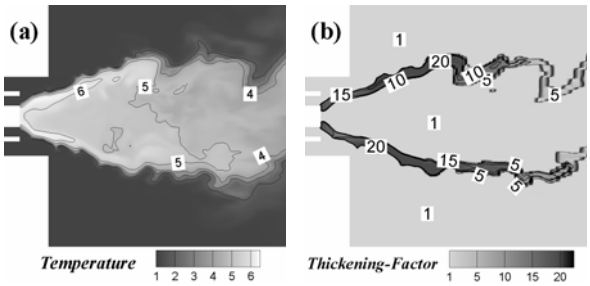

Fig. 3. (a) An instantaneous contour of the temperature, normalized with 298.15K, from R40. (b) thickening-factor F at the same instant.

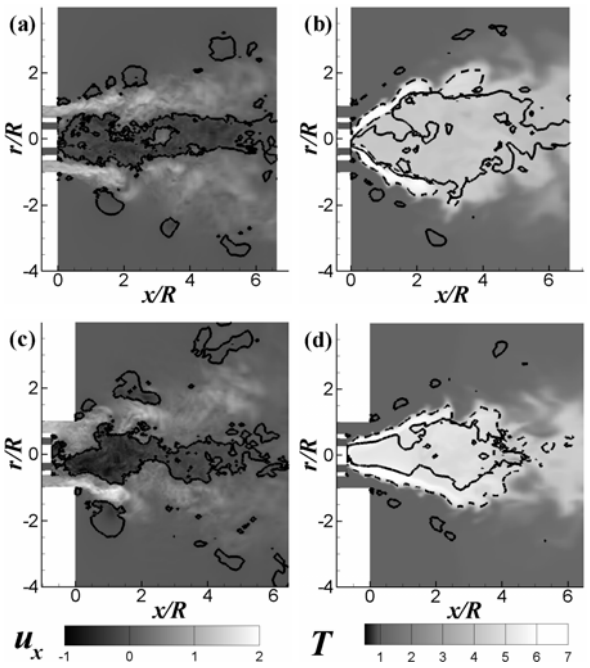

Fig. 4. (a) and (c) instantaneous contours of streamwise velocity, (b) and (d) instantaneous contours of temperature. Solid lines, u_x=0, and dashed lines T=1340K. (a)-(d) are for case I00, R00, I40, R40, respectively. Note: u_x and T are normalized by reference scales, 11.5m/s and 298.15K, respectively.

Behaviour of Recirculation Zone

Instantaneous flowfields obtained in the four cases are shown in Fig. 4, where the recirculation zone is denoted by the zero streamwise velocity contour lines. The CRZs of the two reactive cases (Fig. 4b and 4d) are entirely located in the high temperature post-flame region; hence the local molecular viscosity is substantially higher than in the two non-reactive cases (Fig. 4a and 4c). This explains why the CRZ in the two reactive cases are much smoother than that in the non-reactive ones. Note that the temperature in the case R40 is higher than in the case R00. Unlike the CRZ of cases I00, R00 and R40 (shown in Fig. 4a, 4b and 4c, respectively), the CRZ of case I40 is not stable but precesses regularly around the jet centre. Hence, the instantaneous streamwise velocity at the vicinity of the main jet nozzle oscillates accordingly. This is seen in Fig. 4c, in which higher u_x (brighter colour) is found in the lower side of the jet nozzle and very clear in 3D flowfield animations.

The structures at the outer border of the jets in Fig. 4 show the different spreading angles. This can be quantified with the mean velocity profiles in Fig. 5-8. Taking the profiles at x/R=2 and $r_{1/2}$, the outer point where $\langle u_x \rangle = 0.5 \langle u_x \rangle_{max}$, provides a corresponding measure (Table 1). The behaviour is as follows: when the pilot jet nozzle retracted in the iso-thermal case, the spreading angle increases somewhat, whereas it decreases in the reactive case.

Comparison of Statistical Values

Radial profiles of streamwise and angular velocity statistics for the two non-reactive cases are shown in Fig. 5 and 6. The overall agreement between the LES result and the experimental data (Büchner, 2004) is very good. It is seen that the negative axial velocity region (CRZ) is extended to x/R>3 for I00 (Fig. 5a), while for case I40, it is slightly shorter (Fig. 6a). The profiles of the mean flow show the CRZ, and at the same time, large tangential velocity exists in this region. Downstream turbulence becomes more and more isotropic. The rms fluctuations of angular velocity and streamwise velocity reach the same level, and their profiles become more and more flat.

For the two reactive cases R00 and R40 shown in Fig. 7 and 8, the overall agreement is not as satisfactory as for the non-reactive cases. In the vicinity of the main jet nozzle, x/R=0.l, the agreement for the axial velocity is good. The profile of the tangential velocity of case R40 however differs from the experimental data in the centre region, r/R<0.5. The rms-fluctuations at this station are also under-predicted. Numerous efforts were made to improve the result but failed because of the relatively low grid resolution between the blades of the pilot jet. In the reactive cases, only approximately 12×35 grid cells were used for resolving a single inter-blade channel to keep the total number of points in tangential direction reasonable. For the cases I00 and I40, more grid cells were used. Another source for disagreement is the bias of the LDA data at the outer edge of the jet towards higher velocities since only the jet and not the co-flow was seeded. Finally, a small systematic error occurs in some experimental data reflected by a difference between data from the two sides of the flame, plotted together in these figures.

Sixth International Symposium on Turbulence and Shear Flow Phenomena
Seoul, Korea, 22-24 June 2009

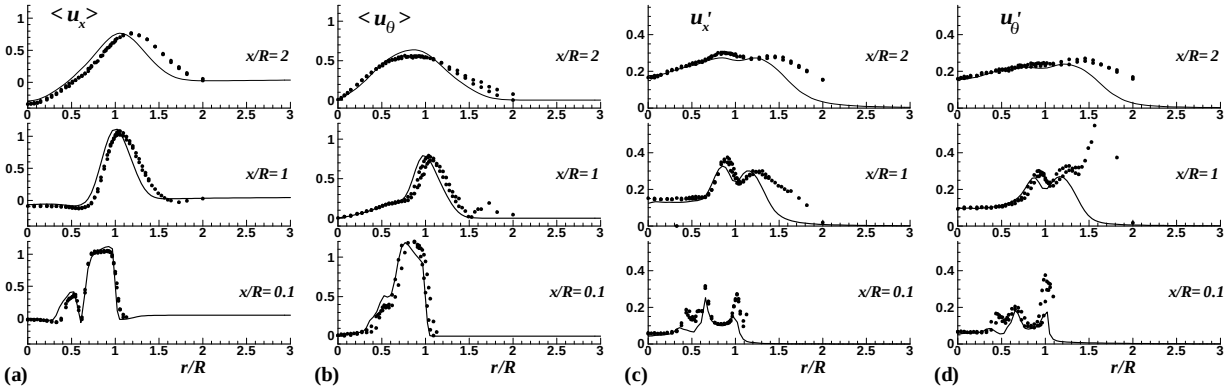

Fig. 5. Radial profiles of velocity statistics for case I00. (a) mean streamwise velocity, (b) mean tangential velocity, (c) rms-fluctuations of streamwise velocity (d) rms-fluctuations for tangential velocity. Symbols: experiment; solid lines: LES results.

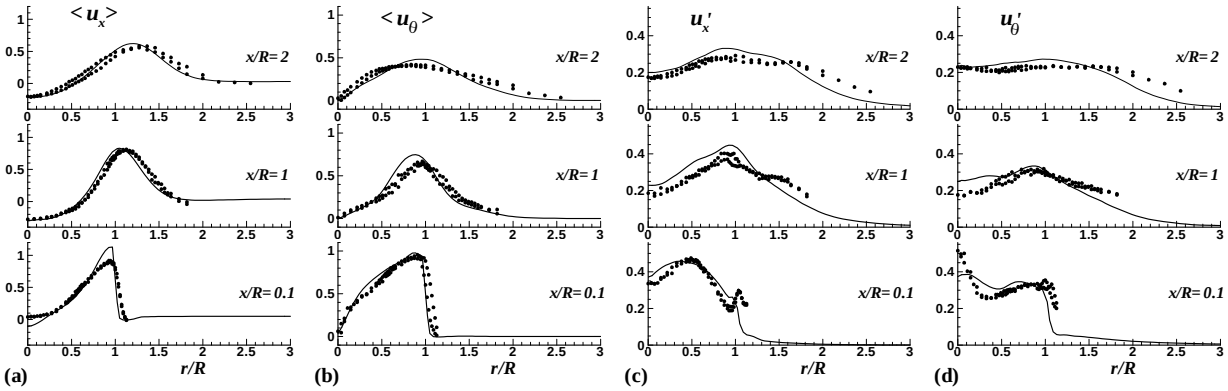

Fig.6. As Fig. 5, but for case I40, iso-thermal retracted setup.

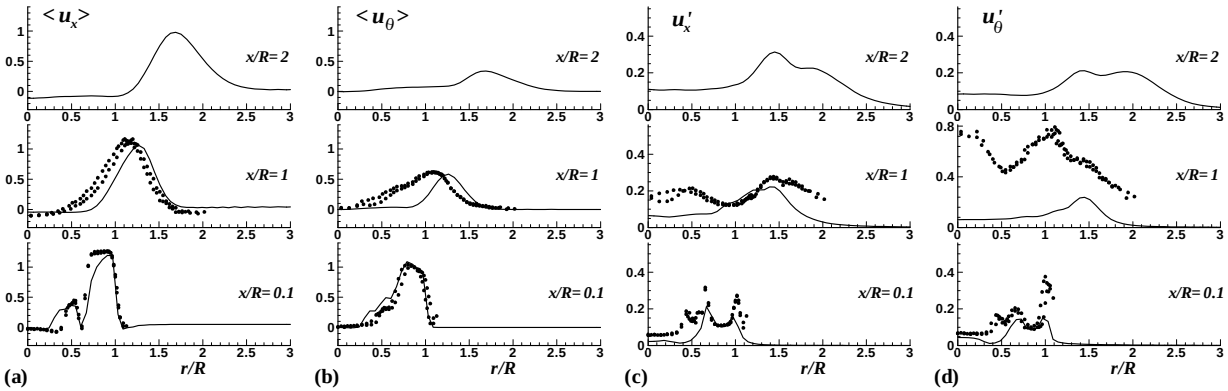

Fig. 7. As Fig. 5, but for case R00, reactive, non-retracted setup.

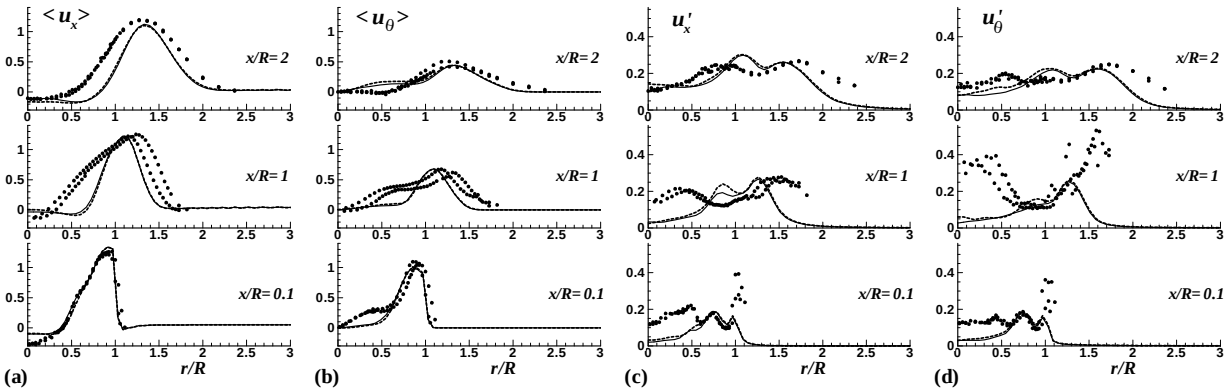

Fig. 8. As Fig. 5, but for case R40, reactive, retracted setup. Symbols: experiment; solid lines: R40; dashed lines: R40B.

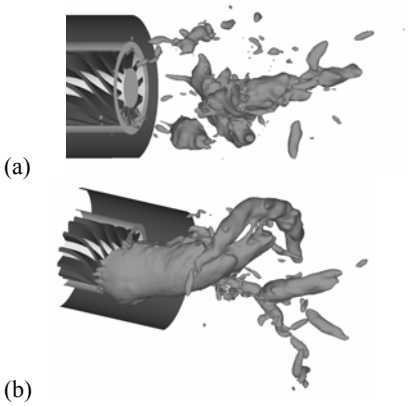

Fig. 9. Smoothed iso-surface of pressure fluctuation, $p-\langle p\rangle=-0.4$. (a) case I00, (b) case I40.

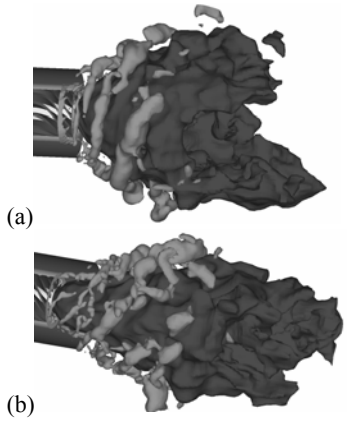

Fig. 10. Smoothed iso-surface of pressure fluctuation in brighter color, $p-\langle p\rangle=-0.1$, and iso-surface of temperature in dark color, $T=1340$ *K*. (a) case R00, (b) case R40.

Coherent Structures

In order to investigate the formation and evolution of coherent structures, iso-surfaces of the pressure fluctuation $p-\langle p\rangle$ are employed, filtered with a 3D box filter of twice the step size of the grid in a post-processing step (Wang, et al., 2008). In Fig. 9b, the PVC in the center region and an induced spiral structure in the outer region are observed together with further small vortex features, rotating around the jet center regularly in the same rotating direction as the PVC. The agreement with the earlier simulations of (Fröhlich, et al. 2008) is excellent. This PVC is not found in case I00, where a big, almost axisymmetric structure is found (Fig. 9a).

Fig. 10 shows vortex structures obtained from the two reactive cases as well as the instantaneous flame front (iso-contour of temperature). The resolved flame front is quite wrinkled. The spiral-type vortices are located outside the flame front. Fig. 10 and numerous other visualizations reveal that large structures with high temperature are only seen far downstream of the nozzle, i.e. for $x/R>2.5$. No big regular vortex structure was found close to the axis at the vicinity of the nozzle, i.e. no obvious PVC exists in the reactive flow. This is due to the fact that the CRZ is fully enclosed in the high temperature post-flame region, as shown in Fig. 4b and 4d.

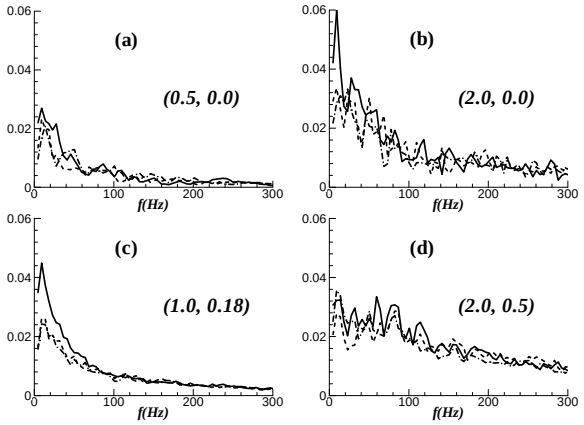

Fig. 11. Power spectrum of velocity components at several points for case I00. The *x*-*r* coordinates of the point where the signal was recorded are given in brackets. Solid lines, streamwise velocity; dashed lines, radial velocity; dash-dot lines, tangential velocity.

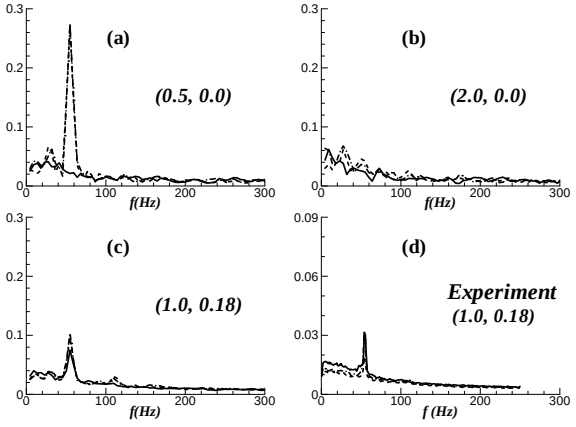

Fig. 12. As Fig. 11, but for case I40.

The only occurrence of PVC in case I40 but not in other three cases is thought to be due to the difference of velocity profiles of them (Syred, 2006). In Fig. 6b at axial station x/R=0.1, a high gradient in the tangential velocity profile is found very close to the centre line. Although high gradients in the tangential velocity are also found in other three cases (Fig. 5b, 7b and 8b), their locations however are little bit more outward.

Power Spectrum Analysis

Power spectra of velocity components at several points are shown in Fig. 11-14. For the non-reactive retracted case (Fig. 12), a dominant peak at f =54Hz, is clearly seen. This frequency is the so-called PVC frequency and coincides very well with the experimental result. For the other three cases, no such dominant peak is found. In these spectra, larger amplitudes generally occur at lower frequency, f<30Hz.

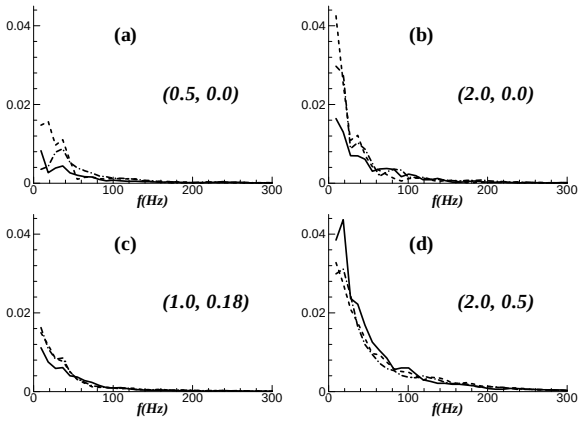

Fig. 13. As Fig. 11, but for case R00.

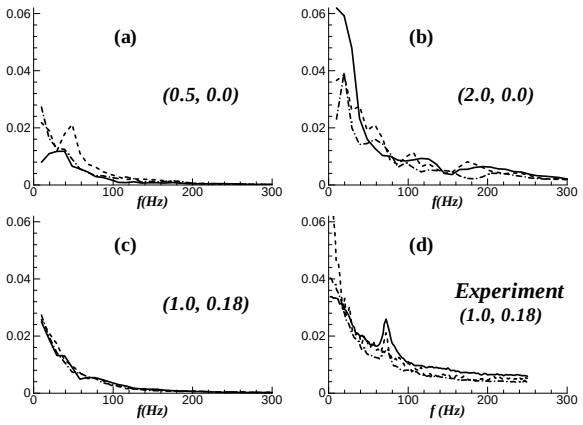

Fig. 14. As Fig. 11, but for case R40.

Quantitative comparison between the LES result and the experimental data is only possible at few points, for instance at position (x/R=1, r/R=0.18), and only for the retracted geometry. Fig. 14d is the experimental result for case R40 at this point, where a small peak at frequency f =71Hz is observed. This peak is missing in the LES, but the overall tendency of the spectra is well predicted (Fig. 14c).

CONCLUSIONS

In this work, the impact of heat release and location of a pilot jet on the swirling flow structures in a co-annular swirl burner is studied with LES. The agreement between the LES results and the corresponding experiment is good. It is demonstrated that strong a PVC only exists in the non-reactive retracted configuration but not in the other three setups, although a CRZ occurs in all the four configurations. When the pilot jet nozzle retracted in the iso-thermal case, the spreading angle increases somewhat, whereas it decreases in the reactive case. The PVC is almost completely suppressed in the cases with reaction where the CRZ is enclosed in the high-temperature post-flame region with low density and high viscosity. This was verified by 3D flowfield visualizations and power spectra of velocity.

ACKNOWLEDGEMENTS

The support of the German Research Foundation (DFG) through the Collaborative Research Center CRC 606 'Unsteady Combustion' is gratefully acknowledged. The computations were performed on both the HP-XC clusters of SSCK Karlsruhe and the SGI Altix 4700 cluster of ZIH Dresden. The authors thank Dr. Büchner and his co-workers (Karlsruhe University) for providing their experimental data in electronic form.

REFERENCES

Büchner, H., 2004, "*Subproject C1: Experimentelle Untersuchungen zur Schwingungsneigung pilotierter Vormischflammen*", Internal report of SFB606: Instationäre Verbrennung: Transportphänomene, Chemische Reaktionen, Technische Systeme, Karlsruhe University.

Colin, O., Ducros, F., Veynante, D., and Poinsot, T., 2000, "A thickened flame model for large eddy simulations of turbulent premixed combustion", *Physics of Fluids*, Vol. 12(7), 1843-1863.

Fröhlich, J., García-Villalba, M. and Rodi, W., 2008, "Scalar mixing and large-scale coherent structures in a turbulent swirling jet", *Flow Turbulence and Combustion*, Vol. 80, 47-59.

García-Villalba, M., Fröhlich, J., and Rodi, W., 2006, "Identification and analysis of coherent structures in the near field of a turbulent unconfined annular swirling jet using large eddy simulation", *Physics of Fluids*, Vol. 18, 055103.

Habisreuther, P., Bender, C., Petsch O., Büchner, H. and Bockhorn, H., 2006, "Prediction of pressure oscillations in a premixed swirl combustor flow and comparison to measurements", *Flow Turbulence and Combustion*, Vol. 77, pp. 147-160.

Legier, J.P., Poinsot, T., and Veynante, D., 2000, "Dynamically thickened flame LES model for premixed and non-premixed turbulent combustion", *Proc. of the summer program*, Center for Turbulent Research, Stanford University.

Lucca-Negro, O, O'Doherty, T., 2001, "Vortex breakdown: a review", *Prog. Energy and Combustion Science*, Vol. 27, 431-481.

Selle, L., Lartigure, G., Poinsot, T., Loch, R., and Schildmacher, K.U. et al., 2004, "Compressible large eddy simulation of turbulent combustion in complex geometry on unstructured meshes", *Combustion and Flame*, Vol. 137, 489-505.

Syred, N., 2006, "A review of oscilation mechanisms and the role of the precessing vortex core (PVC) in swirl combustion systems", *Prog. Energy and Combustion Science*, Vol. 32, 93–161.

Wang, P., Fröhlich, J., Michelassi V., and Rodi, W., 2008, "Large-eddy simulation of variable-density turbulent axisymmetric jets", *Int. J. Heat and Fluid Flow*, Vol. 29, 654-664.

Wang, P., Ayyash, S.K.M., and Fröhlich, J., 2009, "Flame responding to a pulsating pilot jet in an unconfined double-concentric swirl burner", *Proc. of the European Combustion Meeting*, Vienna, Austria.